The final publication is available at

https://doi.org/10.1007/s43032-020-00446-6

Additional Information

Development of Decellularized Oviductal Hydrogels as a Support for Rabbit Embryo Culture

Emilio Francés-Herrero[1,2], Lucía De Miguel-Gómez[1,2], Sara López-Martínez[1], Hannes Campo[1,3], Ximo Garcia-Dominguez[4], Gianfranco Diretto[5], Amparo Faus[1], José S. Vicente[4], Francisco Marco-Jiménez[4], Irene Cervelló[1]

[1] Fundación Instituto Valenciano de Infertilidad (FIVI), Instituto de Investigación Sanitaria La Fe, Avenida Fernando Abril Martorell,
    106. Hospital La Fe, Torre A, Planta 1ª, 46026 Valencia, Spain

[2] Universitat de València, Valencia, Spain

[3] Division of Reproductive Science in Medicine, Department of Obstetrics and Gynecology, Feinberg School of Medicine, Northwestern University, Chicago, IL 60611, USA

[4] Universitat Politècnica de València, Valencia, Spain

[5] Italian National Agency for New Technologies, Energy and Sustainable Development, Rome, Italy

Abstract

The oviducts (fallopian tubes in mammals) function as the site of fertilization and provide necessary support for early embryonic development, mainly via embryonic exposure to the tubal microenvironment. The main objective of this study was to create an oviduct- specific extracellular matrix (oviECM) hydrogel rich in bioactive components that mimics the native environment, thus optimizing the developmental trajectories of cultured embryos. Rabbit oviducts were decellularized through SDS treatment and enzymatic digestion, and the acellular tissue was converted into oviductal pre-gel extracellular matrix (ECM) solutions. Incubation of these solutions at 37 °C resulted in stable hydrogels with a fibrous structure based on scanning electron microscopy. Histological staining, DNA quantification and colorimetric assays confirmed that the decellularized tissue and hydrogels contained no cellular or nuclear components but retained important components of the ECM, e.g. hyaluronic acid, glycoproteins and collagens. To evaluate the ability of oviECM hydrogels to maintain early embryonic development, two-cell rabbit embryos were cultured on oviECM-coated surfaces and compared to those cultured with standard techniques. Embryo development was similar in both conditions, with 95.9% and 98% of the embryos reaching the late morula/early blastocyst stage by 48 h under standard culture and oviECM conditions, respectively. Metabolomic analysis of culture media in the presence or absence of embryos, however, revealed that the oviECM coating may include signalling molecules and release compounds beneficial to embryo metabolism.

Keywords Decellularization · Hydrogel · Oviduct · Fallopian tubes · ECM · Embryo culture

Introduction

Infertility is a disorder of the reproductive system defined by the World Health Organization as "the failure to achieve a clinical pregnancy after 12 months or more of regular unprotected sexual intercourse". Currently, around 15% of couples worldwide experience infertility and, for many of them, assisted reproductive technologies (ARTs) provide a helpful alternative [1]. This field and, in particular, in vitro embryo culture have improved significantly over the last de- cades, with a multitude of chemical formulations and physical platforms for culture being developed [2]. Even so, current embryo culture techniques are far from ideal, as in vitro con- ditions fail to mimic the physiological dynamics within the reproductive tract. The female reproductive tract has complex hydrated surfaces coated with macromolecules, hydroxylated compounds, growth factors and components of the extracellu- lar matrix (ECM). This is in stark contrast with the inert cul- ture surfaces currently in use, e.g. glass, polystyrene and poly- dimethylsiloxane [3]. This could be a contributing factor to the developmental gaps exhibited in in vitro cultured mammalian embryos, reducing ART success rates [4–6].

Bioengineering based on the ECM may help solve this problem. The ECM plays vital roles in many organ systems, and decellularized tissues that harness the intrinsic qualities of the ECM have many possible applications. A major example is the creation of bioengineered patches to regenerate dam- aged tissues. This approach has been implemented with prom- ising results in the management of the uterus [7–10], vagina [11, 12] and ovary [13, 14]. Further, unique tissue-specific ECM hydrogels have been derived from virtually all major tissues and organs [15–20], including reproductive tissues such as the endometrium [21]. Because of their composition and three-dimensional organization similar to native tissues, they have been successfully used for regenerative and other biomedical purposes [22]. Of note, decellularization is partic- ularly advantageous as it removes all cellular material and epitopes allowing both allogeneic and xenogeneic sources to be used [23, 24], facilitating throughput and adoption in a clinical setting.

In terms of ART, decellularized tissue could be used to improve culture systems. The biophysical and chemical cues of embryonic microenvironments impart significant spatio- temporal effects on development [25, 26]. Tissue engineering could be used to recreate these microenvironments by devel- oping advanced in vitro embryo culture platforms incorporat- ing different biomaterials, media and mechanical forces [6]. Synthetic or nonspecific naturally derived hydrogels such as gelatin, laminin or collagen are commonly used to culture embryos or embryonic stem cells [27–32]. Decellularized tis- sues, on the other hand, have potential advantages due to their specific structures, intrinsic biological activity and complex biochemical characteristics. Decellularized ECM is primarily composed of structural proteins, such as collagen, elastin and laminin, and glycosaminoglycans (GAGs), but it can also con- tain nontrivial concentrations of endogenous growth factors, secretions and matrix-bound nanovesicles [33–35]. Such ECM components can influence embryo development by reg- ulating the activity of signalling pathways and supplying spe- cific biomolecules and cytokines to the medium [36]. Thus, using tissue-specific ECM hydrogels as in vitro coatings [15] is a promising way to achieve reliable embryo culture [21].

In this study, the first of its kind, we examine the proteome, GAGs and hyaluronic acid (HA) composition of a pre-gel solution derived from decellularized rabbit oviducts and test its ability to support the development of rabbit embryos. Our goal was to create an oviduct-specific extracellular matrix (oviECM) hydrogel rich in bioactive components capable of mimicking the natural microenvironment in which preimplan- tation embryos develop. Fallopian tubes, or oviducts, were chosen as the source tissue as these

2

structures are essential for successful spontaneous conception in humans and facili- tate early embryo development, allowing embryos to reach the uterine cavity and implant in a receptive endometrium [37]. The hypothesis is that oviductal hydrogels will facilitate early embryo development in culture, eventually improving im- plantation and normal intrauterine pregnancy.

Material and Methods

Study Design

After 72 h of ovarian stimulation, oviducts (n = 24) were iso- lated from twelve rabbits. Eighteen oviducts were decellularized in three pools (n = 6 per pool) and 6 kept as the control group. The decellularization efficiency was tested (see below), and the resulting acellular tissue was milled and lyophilized. Pre-gel solutions were made by partially digesting ECM powder and control tissue powder. The solu- tions were aliquoted and stored at −80 °C until use. The de- rived hydrogels were characterized by scanning electron mi- croscopy (SEM), proteomics and quantification of GAGs and HA. The biological activity of the oviductal ECM— oviECM—hydrogels was studied by culturing day-1 rabbit embryos for 48 h in two different conditions: on a surface coating made from acellular oviduct hydrogels (CM + OH + E) and in standard culture conditions (CM + E). The develop- mental rate of the embryos and metabolites in the media was analysed. Figure 1 shows a complete outline of the methodology.

Animal Setting

New Zealand White rabbits housed at the Universitat Politècnica de València experimental farm were used. Mating-induced ovulation in this species makes it possible to precisely pinpoint embryonic age, and these animals are widely used to study reproduction [38]. The animals were kept in flat deck indoor cages, with free access to food and water. All experimental procedures were performed in accordance with Directive 2010/63/EU EEC for animal experiments and reviewed and approved by the Ethical Committee for Experimentation with Animals of the Polytechnic University
of Valencia, Spain (research code: 2018/VSC/PEA/0116).

Oviduct Decellularization

Ovulation was induced in twelve rabbits using hormonal treat- ment consisting of 1 μg of Buserelin acetate (Hoechst Marion Roussel S.A., Madrid, Spain). After 72 h, oviducts (n = 24) were isolated. Before decellularization, surrounding fat was removed and the oviducts were washed with PBS, cut into 5-mm pieces and separated into 4 pools (n = 6 oviducts per pool): three to be independently decellularized and one to remain as an untreated control. Decellularization was per- formed via a 2-day SDS-based protocol and agitation with a magnetic stirrer at 300 RPM (Table 1). Briefly, oviduct pools were subjected to chemical detergents (SDS, Triton X-100; Sigma-Aldrich), an enzymatic solution (DNase 1 (D4513- 1VL), diluted in 1.3 mM MgSO4 and 2 mM CaCl2; Sigma-Aldrich) and PBS washes (Thermo Fisher Scientific).

Assessment of Decellularization Efficiency of Oviducts: Histological Analysis and DNA Quantification

Decellularized oviducts and native tissues were fixed over- night with 4% paraformaldehyde (PFA; Sigma-Aldrich) at 4 °C then dehydrated in graded alcohol/xylene, embedded in paraffin and sectioned on a microtome (HM 310, Microm). The 4-μm sections were mounted onto glass slides (Superfrost Plus, Thermo Scientific).

Haematoxylin and eosin (H&E), Alcian blue (AB) and Masson's trichrome (MT) stains were used to assess the presence of cellular components, sulphated GAGs and collagen, re- spectively. To detect nuclear DNA, mounting medium containing 6-diamidino-2-phenylindole (DAPI; Thermo Fisher Scientific) was used. All images, for both bright- field microscopy and fluorescence microscopy, were taken with a Nikon Eclipse 80i microscope. Following lyophilization of the control tissue and ECMs (see below), DNA was extracted from 12 mg samples using the DNeasy Blood & Tissue kit (Qiagen) following the man- ufacturer's instructions. The DNA yield (ng/µl) was quanti- fied using the NanoDrop One® (Thermo Scientific).

Preparation of Cellular and Acellular Oviductal Matrix Hydrogels

Decellularized and native oviduct fragments were frozen in liquid nitrogen, ground in a mortar and stored at −80 °C.

The resulting powder was lyophilized (LyoQuest -85, Telstar) for 48 h at 20 Pa and −80 °C and finally stored at −20 °C. Acellular and control tissue hydrogels were created using a modified protocol [39] that conserves the ECM. Lyophilized powder was suspended at 1% (w/v) in 0.01 M HCl (Sigma- Aldrich) with 0.1% (w/v) pepsin (Sigma-Aldrich) and digested for 48 h at room temperature with constant agitation using a sterilized magnetic stirrer. The solution was iced, and digestion stopped by neutralization to physiological pH with 10% (v/v) 0.1 M NaOH (Sigma-Aldrich) and 10% (v/v) 10× PBS. The resulting pre-gel solution was aliquoted and stored at −80 °C; this solution forms a stable hydrogel at 37 °C.

Hydrogel Characterization: Fibre Size, Sterility, and GAGs and HA Quantification

Ultrastructural assessment and fibre size analysis were per- formed via SEM. Pre-gel solutions were left to gel for 20 min at 37 °C. Gels were fixed in 2.5% glutaraldehyde in PBS (Sigma-Aldrich, grade II, 25%) at 4 °C overnight, slowly critical point dried, coated with gold-palladium for 2 min using an SC7640 Sputter Coater (Quorum Technologies) and imaged with a Hitachi S-4800 SEM FEG. Native micro- scope software was used to measure fibre diameters.
GAGs and HA were quantified in pre-gel solutions from both decellularized and control tissues. The Blyscan™ Glycosaminoglycan Assay and the Purple-Jelley Hyaluronan Assay (Biocolor) kits were used according to the manufac- turer's instructions to extract and stain GAGs and HA, respec- tively. Yields were measured spectrophotometrically, using a SpectraMax 190 Microplate Reader (Molecular Devices, USA).
To test sterility and structural stability, oviECM hydrogels were incubated in SAGE 1-Step™ medium (CooperSurgical) for 4 days at 37 °C and 5% CO2.

Proteomic Analysis

Native and decellularized oviductal pre-gel solutions (10 µg/ µl) were used, with 100 µg of each sample being loaded and resolved on a one-dimensional SDS-PAGE gel. Each sample lane was sliced into 5 fragments and digested with sequencing grade trypsin (Promega) as described [40]. Trypsin digestion was stopped with trifluoroacetic acid at a final concentration of 10%, and the supernatant (SN) was removed. The library gel slides were dehydrated with pure acetonitrile (ACN). The new peptide solutions were combined with their correspond- ing SNs. The peptide mixtures were dried in a speed vacuum and resuspended in 2% ACN and 0.1% TFA.
For liquid chromatography and tandem mass spectrometry (LC-MS/MS), peptides were loaded onto an analytical column (LC column, Luna Omega 3 µm Polar C18, 150 mm ×

0.3 mm, Capillary Phenomenex) and analysed in a microESI qQTOF (TripleTOF 6600plus, AB SCIEX) spectrometer.

For protein identification in each sample, the MS/MS spec- tral files of the sample's 5 gel fragments were combined. ProteinPilot default parameters were used to generate peak lists directly from TripleTOF 6600plus wiff files. The Paragon Algorithm [41] of ProteinPilot v 5.0 was used to search the UniprotMammals database (version 03-2018) with the following parameters: trypsin specificity, IAM Cys alkyl- ation, taxonomy not restricted and the search effort set to through. The Pro group algorithm was used for protein group- ing. Proteins showing unused scores >1.3 were identified with confidences ≥95%.

To perform differential abundance analysis, a spectrum li- brary was built. Data from each fragment type were combined in a search for all samples, and ProteinPilot v 5.0 was used to generate a peak list and to search the UniprotMammals data- base. As above, the Pro group algorithm was used for protein grouping. Subsequently, PeakView 1.1 (Sciex) was used to quantify the areas for the peptides assigned in the library (maximum 100 peptides per protein). Only peptides with con- fidences ≥95% were quantified. Shared or modified peptides were not quantified. The protein areas determined for every fragment were exported by MarkerView 1.3.1 (Sciex), com- bined in a single matrix and normalized by the summed total areas.

In Vitro Embryo Culture

Eight New Zealand White rabbits were used as embryo donors in 2 separate experiments (n = 4 rabbits per experiment). Ovarian stimulation was induced using 3 µg of long-acting follicle-stimulating hormone (Corifollitropin alfa; Elonva, Merck Sharp & Dohme S.A., Spain) as described previously [42]. Seventy-two hours later, ovulation was induced via an intramuscular injection of 1 µg buserelin acetate (Suprefact; Hoechst Marion Roussel, S.A., Madrid, Spain). Females were inseminated with a heterospermic pool of semen to randomize male effect and, 24 h later, were euthanized. Two-cell embry- os were collected at room temperature by flushing the ovi- ducts and uterine horns with Dulbecco's phosphate-buffered saline (DPBS), supplemented with 0.2% (w/v) bovine serum albumin (BSA) and antibiotics (penicillin G sodium 60 IU/ml, penicillin G procaine 140 IU/ml and dihydrostreptomycin sul- phate 0.250 mg/ml; Penivet 1; Divasa Farmavic, Barcelona, Spain) and pooled to randomize donor effect. Pools of 24–25 embryos were cultured in 4-well Nunc plates (Thermo Fisher Scientific) for 48 h at 38.5 °C, 7% CO2 and saturated humid- ity. Two different conditions were tested: (i) SAGE 1-Step™ HSA medium (CooperSurgical), 148 embryos, and (ii) oviECM coating with SAGE 1-Step™ medium, 150 embryos. To coat the wells, 250 µl of ECM pre-gel solution was added and left overnight at 4 °C to allow nonspecific adherence of proteins. The coating solution was then aspirated, and the wells were rinsed once with PBS before adding the culture medium.

Metabolomic Analysis

Four experimental conditions were analysed by metabolo- mics: (i) SAGE 1-Step™ medium incubated for 48 h (CM), (ii) SAGE 1-Step™ medium that was in contact with an oviECM coating for 48 h (CM + OH), (iii) SAGE 1-Step™ medium in which embryos were grown for 48 h (CM + E) and (iv) SAGE 1-Step™ medium in which embryos were grown on an oviECM coating for 48 h (CM + OH + E). Targeted and untargeted LC-ESI(+/−)-MS analysis of the semi-polar metabolome (consisting of water-soluble molecules) of the media was performed as previously described [43–45]. Semi-polar metabolites were extracted from 250 µl lyophilized medium with 0.75 ml of cold 75% (v/v) methanol and 0.1% (v/v) formic acid, spiked with 10 µg/ml formononetin as an internal standard. Samples were shaken for 40 min at 20 Hz using Mixer Mill 300 (Qiagen) then

centrifuged for 15 min at 20,000×g at 4 °C. Supernatants (0.6 ml each) were transferred to HPLC tubes. For each experimental group, 6 independent biological replicates were analysed, with at least one technical replicate for each. Liquid chromatography (LC) was per- formed on 5 µl of each sample with a Phenomenex C18 Luna column (100 × 2.0 mm, 2.5 µm) and a flow rate of 0.25 ml/min throughout. The mobile phase was composed of solutions A (water-0.1% formic acid) and B (ACN-0.1% formic acid) in a linear gradient from 95% A:5% B (1 min) to 25% A:75% B over 40 min, then 2 min isocratic, followed by a return to the initial LC conditions over 18 min.

Mass spectrometry analysis was performed using a quadrupole-Orbitrap Q Exactive system (Thermo Fisher Scientific, USA) operating with positively/negatively heat- ed electrospray ionization (HESI) or atmospheric pressure chemical ionization (APCI) coupled to an Ultimate HPLC- DAD system (Thermo Fisher Scientific, Waltham, MA, USA). For metabolite analysis, mass spectrometer parameters were as follows: capillary and vaporizer temperatures of 30 °C and 270 °C, respectively, 4.0 kV discharge cur- rent, 370 °C probe heater temperature and a 50 V S-lens RF level. The acquisition was carried out in the 110/ 1600 m/z scan range, with the following parameters: reso- lution 70,000, microscan 1, AGC target 1e6 and maximum injection time of 50 ms. Full-scan mass spectrometry (MS) with data-dependent MS/MS fragmentation was used to identify metabolites. All solvents used were LC-MS grade quality (CHROMASOLV® from Sigma-Aldrich). Metabolites were quantified in a relative way by normalization to internal standard (formononetin and DL-α-to- copherol acetate) amounts.

Bioinformatics and Statistics

Exploratory analysis of proteomic data was performed using ClustVis online software (https://biit.cs.ut.ee/clustvis/). Serum albumin, keratins and trypsin were considered contaminants and were excluded from analysis. Differential abundance was evaluated using the moderate t statistic from the R limma package (p values adjusted by the Benjamini-Hochberg meth- od [46]). The functional enrichment analysis was performed with the over-representation analysis method implemented in the Panther database (http://geneontology.org). Proteins annotated with Gene Ontology terms GO: 0005576 (extracellular region), GO: 0005615 (extracellular space), GO: 0005886 (plasma membrane) and GO: 0009986 (cell surface) were classified as extracellular proteins. The STRING database (version 10) was used for protein-protein interaction analysis, and MatrisomeDB 2.0 (http://www. matrisomedb.org) was used to identify matrisome annotations [47].

Untargeted metabolomics was performed using the SIEVE software (Thermo Fisher Scientific). Differentially accumulated metabolites (DAMs) were identified by a t test with correction for multiple comparisons using the Holm-Sidak method [48] using GraphPad Prism (GraphPad Software, Inc., CA, USA). Targeted metabolite identification was performed by comparing chromato- graphic and spectral properties with authentic standards (if available) and reference spectra, an in-house database and literature data, and on the basis of the m/z accurate masses, as reported in the PubChem database or on the Metabolomics Fiehn Lab Mass Spectrometry Adduct Calculator. Targeted DAMs were identified by one-way ANOVA plus Tukey's pairwise comparison using the SPSS software (SPSS, Inc., Chicago, IL, USA). Quantitative data were expressed as the mean value ± stan- dard deviation (SD). Unpaired t tests were used to identify any significant differences in fibre sizes, DNA, GAGs and HA levels and embryo development rates. The data were analysed using SPSS (SPSS, Inc., Chicago, IL, USA). A p value ≤0.05 in a two-tailed test was considered statistically significant.

Results

Macroscopic and Histologic Analysis and DNA Quantification of Decellularized Rabbit Oviducts

During the decellularization process, the oviduct fragments changed from red to white and became semi-transparent. The samples preserved their tubular structure, and there was a visible reduction in the surrounding fat (Supplementary Fig. 1a, c). Decellularization was first confirmed by histolog- ical methods. Based on H&E and DAPI stains, the bioengineered oviductal scaffolds were devoid of cellular and nuclear material (Fig. 2a–d). DNA was quantified, and a significant reduction was observed after decellularization (4958.65 ± 141.61 ng/mg dry tissue weight in control samples compared to 161.18 ± 32.18 in decellularized samples, N =3 per group, p = 0.000) (Fig. 2i). Histochemical assessments demonstrated preservation of the ECM architecture and content. Masson's trichrome stain- ing showed that collagen fibres, a major ECM component, remained after decellularization (Fig. 2e, f); however, Alcian blue staining revealed a reduction in GAGs, with a faint signal being appreciable (Fig. 2g, h).

Hydrogel Preparation and Characterization: Biochemical Properties and Ultrastructure

Native tissue and decellularized ECM were lyophilized and digested by pepsin (Supplementary Fig. 1a–e). The resulting pre-gel solutions formed stable gels when left at 37 °C for 20 min (Supplementary Fig.1f). Long-term struc- tural stability and sterility of the ECM-derived gels were demonstrated by incubation at 37 °C in the SAGE 1-Step™ culture medium for 4 days. The hydrogel remained intact during this period, and no bacterial growth was observed (data not shown). SEM was used to assess the ECM ultrastructure in hydrogels from native and decellularized tissues. The hydrogels had similar complex fibre networks based on low- and high-magnification images. In both cases, the typical D- periodicity of collagen fibres was seen (Fig. 3a–h). Fibre di- ameters were analysed from ×100,000 images (>30 measure- ments per hydrogel), measuring on average 38.32 ± 5.97 nm and 36.13 ± 6.03 nm in control and oviECM hydrogels, re- spectively (Fig. 3k).

To further assess the effect of decellularization and solubi- lization on GAGs, a colorimetric kit for GAGs in general and one specifically for HA were used. The concentration of GAGs was significantly reduced after decellularization (from 99.49 ± 8.20 µg/ml in control hydrogels to 15.38 ± 0.41 µg/ml in hydrogels from decellularized tissue, N = 3 per group, p = 0.000) (Fig. 3i). Interestingly, HA, a non-sulphated anionic glycosaminoglycan present in some specialized culture media for embryonic culture, did not exhibit such a drastic decrease (3.55 ± 0.10 µg/ml in control hydrogels compared to 2.53 ± 0.25 µg/ml in hydrogels from decellularized tissue, N = 3 per group, p = 0.0029) (Fig. 3j). This indicates SDS and pepsin treatments have a less dramatic effect on this specific GAG.

Hydrogel Proteome Analysis

After demonstrating the retention of collagens, we studied how decellularization affects the overall protein composition of the resulting hydrogels. Based on SDS-PAGE, hydrogels from decellularized tissue are enriched in high molecular weight proteins (Fig. 4a). Using MS, we quantified 399 com- mon proteins in three biological replicates of each hydrogel. In both clustering (Fig. 4b) and principal component analysis (Supplementary Fig. 2), a clear separation was observed be- tween the two experimental groups. Differential abundance analysis confirmed the exploratory heatmaps and revealed that a large proportion of the proteins were more abundant in na- tive hydrogels, with only a few proteins found to be enriched in oviECM hydrogels (171 vs. 6, respectively).

Gene ontology (GO) analysis was performed for proteins with statistically significant differential abundance. Proteins enriched in oviECM hydrogels related to extracellular micro- fibrils or desmosomes, while other ECM proteins (collagens and laminins) and those relating to the cytoplasm, cell organ- elles and nucleus were highly enriched in native hydrogels (Fig. 4c). In terms of molecular function, hydrogels from acel- lular tissue contained a high percentage of ECM constituents conferring elasticity, whereas native hydrogels contained prin- cipally proteins involved in catalytic and substance exchange. A further GO analysis of biological processes showed that proteins in charge of maintaining the position of other proteins in the extracellular space were significantly enriched in oviECM hydrogels, while proteins involved in signal trans- duction and sugar and lipid metabolism predominated in na- tive hydrogels. Supplementary Fig. 3 shows the results of a GO enrichment analysis carried out with all the proteins iden- tified in the oviECM hydrogels.

Many of the observations obtained through over- representation analysis (ORA) were verified by protein- protein interaction analysis carried out using the STRING database (Supplementary Fig. 4). A network comprising 100 proteins with the most significant differential abundances re- vealed functional enrichments of ontologies very similar to those described above.

To better characterize extracellular proteins in both hydrogels, the proteomic data were mapped onto the matrisome database (MatrisomeDB 2.0) [49], where matrisomal proteins are divided into the 'core matrisome' (encompassing glycoproteins, collagens and proteoglycans) and the 'matrisome-associated proteins' (encompassing affil- iated proteins, regulators and secreted factors). In this analysis, only qualitative data for proteins showing unused scores >1.3 and present in at least 2 of the 3 biological replicates from each experimental condition were considered. The oviECM hydrogels had larger proportions of collagens, glycoproteins, ECM-affiliated proteins, ECM regulators and secreted factors than the native hydrogels (Fig. 5a). Of note, 68% of the extra- cellular proteins in the oviECM hydrogels were matrisomal, whereas only 35% were matrisomal in native hydrogels. However, the absolute number of proteins from all matrisomal categories (excepting collagens) was higher in native hydrogels (Fig. 5b). This indicates that some matrisomal pro- teins have been lost during decellularization. However, the extracellular fraction has been enriched. A list of the matrisomal proteins of both hydrogels is shown in Table 2.

Effect of oviECM Hydrogel Coating on In Vitro Embryo Development and Metabolism

Embryos were cultured under standard conditions or on plas- tic coated with oviECM hydrogels. Embryo development was similar in both conditions, with 95.9% and 98% of the embry- os reaching the late morula/early blastocyst stage by 48 h un- der standard culture and oviECM conditions, respectively. The morphology and appearance of the embryos were also similar in both conditions (Supplementary Fig. 5).

Metabolites in negative control media (with and without oviECM coating; CM + OH and CM, respectively) and media with embryos (with and without oviECM coating; CM + OH + E and CM + E, respectively) were compared by targeted and untargeted LC-ESI(+/−)-MS analysis of the semi-polar metabolome. Base peak alignment of chromatograms re- vealed appreciable differences between the ion populations of the four conditions (Supplementary Fig. 6). Once filtered, the untargeted data of 50 metabolites re- vealed explicit differences in the compositions of the different media. Exploratory analysis of the results (PCA and heatmap) identified two large groups among the 24 samples analysed (6 per condition): one characteristic of the CM condition and one characteristic of the other three conditions (Fig. 6a, b). This information is consistent with the number of DAMs found when comparing the conditions. Culturing of embryos for 48 h under

standard or oviECM conditions changed the base- line composition of the media in regard to 17 and 1 metabolite, respectively (Fig. 6c). Likewise, simply supplementing the culture medium with the ECM pre-gel solution in the absence of embryos revealed 17 DAMs. This indicates that, to reach a similar end point (4 DAMs were detected between the CM + E and CM + OH + E conditions), there is less change during embryo culture when oviECM coating is present, implying that embryos need to acclimatize less than they do under standard culture conditions.

Targeted analysis focused on metabolites associated with energy metabolism (glycolysis and oxidative phosphorylation) and amino acid biosynthesis of the embryos due to the importance of these metabolic pathways in early embryonic development. A total of 20 metabolites in these pathways could be detected, 11 of which exhibited differential abundance in some conditions (Table 3). When the embryos were cultured on an oviECM hydrogel coating, consumption of almost all identified amino acids as well as glucose and glycolysis intermediates was observed but the differences in metabolite abundances were not significant after 48 h of embryo culture. Interestingly, incubating just the oviECM coating in culture medium increased the levels of amino acids and glycolysis intermediates, indicating the oviECM hydrogel provides these compounds, which could be used by the embryos. To meet a comparable end state, under standard culture conditions, the embryos significantly produced and released amino acids and intermediates from glycolysis, consuming glucose and gluconate. Additionally, in oviECM culture conditions, the turnover of the 15 identified amino acids was half that of standard culture conditions (data not shown).

Discussion

The ECM, a tissue-specific network made up of fibrous pro- teins, proteoglycans and GAGs, provides three-dimensional structural support for cells and possesses signalling cues and bioactive components [50]. This enables cells to differentiate and maintain their functions and phenotypes in a specialized local microenvironment [51]. The ECM is dynamic, undergoes continuous remodelling and is carefully regulated, starting from the earliest phases of embryonic development [52–54]. For ex- ample, laminin is already expressed by 16-cell stage murine embryos and collagen IV in early blastocysts [55].

ECM hydrogels have been derived from almost all human tissues and organs since the first report of a crude decellularization technique more than 70 years ago [23, 56, 57]. These biocompatible hydrogels can promote cell differentiation, or they are better than other substrates such as Matrigel or purified ECM components, such as collagen [58, 59]. Hydrogels have already been used in preclinical applica- tions for the treatment of ulcerative colitis [60], traumatic brain injury [61] and stroke [62]. Moreover, xenogeneic decellularized tissues are being approved for use in humans by the Food and Drug Administration (FDA) [63]. In terms of reproductive medicine, hydrogels made from the oviduct could provide the conditions naturally occurring in the female reproductive tract during early embryo development [64].

To create a culture environment to mimic the oviduct, we chose the rabbit as an animal model given its phylogenetic closeness to humans, the size of its oviducts and its reproduc- tive performance [38]. Using our prior experience [21, 65], we adapted a decellularization protocol using Triton X-100 and SDS. These widely used chemical compounds, in combina- tion with enzymatic treatments, can provide an optimal bal- ance between the removal of cellular and antigenic material and the preservation of native ECM structure and composition [23]. Consistent with this, our histological analysis revealed complete removal of cellular and nuclear material but the maintenance of a dense network of collagen fibres in our decellularized oviducts. Further DNA

quantification con- firmed the elimination of the majority of nucleic material in our decellularized tissue, which had only 3.25% (w/w) of the DNA found in native tissue.

The surface of the female reproductive tract is coated with polyhydroxylated compounds, macromolecules and compo- nents of the ECM. The latter are mainly differentiated into two groups: GAGs and fibrous proteins [66]. Alcian blue staining and colorimetric quantification demonstrated moder- ate retention of GAGs in our oviECM hydrogels. GAGs are important mediators between cells and their environment. They control the diffusion of macromolecules and the interac- tion of cells with a variety of ligands (e.g. growth factors and hormones) [67]. Moreover, GAGs are intrinsically abundant in follicular, oviductal and uterine fluids and it was demon- strated that they support the proliferation and differentiation of embryonic cells [68]. Because of this, it is possible that they may facilitate the development of in vitro fertilization (IVF) oocytes to blastocyst stage in vitro. We did observe excellent retention of a specific GAG, HA, within oviECM hydrogels. The addition of HA to culture media has been shown to im- prove blastocyst development in IVF-derived bovine embryos [69–71] and is a suitable substitute for serum proteins for supporting mouse blastocyst development [72].

Quantitative analysis of the protein composition of our native and ECM oviductal hydrogels showed a general decrease in protein abundance after the decellularization process. The partial removal of cellular proteins was demonstrated by the decreased level of proteins involved in metabolic processes, synthesis and exchange of substances (ions and <1000 Da molecules). Furthermore, GO enrichment of the proteins identified in these hydrogels revealed that collagen fibrils, desmosomes, basement membrane and ECM components are among the most enriched cellular component GO terms. When comparing the proteome profile to previously published endometrial hydrogels by our group [21], we saw a high similarity within the structural ECM proteins present; however, more than 50% of the detected proteins were different between both. More precise proteomic methods could elucidate these differences deeper. We also char- acterized the ECM protein signatures (matrisomes) of the gen- erated hydrogels. Although more matrisomal proteins were identified in the native hydrogels, they accounted for only 35% of the total extracellular proteins compared to 68% in the decellularized hydrogel. Various ECM compounds have been shown to influence the in vitro growth, function and differenti- ation of various adherent somatic cells [73] and may influence the development of preimplantation embryos. For example, fi- bronectin added to culture media supported mouse embryo de- velopment but did not improve the development achieved with control treatments [72]. However, both fibronectin and laminin, which are present in our oviECM hydrogels, can improve hu- man blastocyst hatching rates [74]. Furthermore, laminin has been described to bind to growth factors with high affinity [75]. Culturing day-1 embryos on our oviECM coating did not improve classic markers of embryonic viability (blastocyst development rate, morphology and appearance); however, it might have assisted embryo metabolism. The metabolism of preimplantation embryos can reveal distinctive characteristics associated with their development and implantation potential [76]. Our untargeted metabolomic analysis revealed that when the oviECM coating was used, the starting culture composi- tion resembled its final composition. This implies that the embryos required less acclimatization and expended less en- ergy in creating an optimal environment for their develop- ment. In the same vein, targeted metabolomic analysis showed that under CM conditions, the embryos significantly produced and released amino acids and intermediates from glycolysis, consuming glucose and gluconate. However, the oviECM hy- drogel seemed to provide amino acids and glycolysis interme- diates to the medium, which could then be used by the embryos in low amounts.

We believe our results are most consistent with the "quiet embryo hypothesis", which proposes that unstressed viable preimplantation embryos operate at lower metabolite or

nutri- ent turnover rates than those of their less viable counterparts [77]. Hamatani et al. [78] described two physiological states of blastocysts (activation and dormancy) according to the global expression of genes involved in energy metabolism, cell signalling and cell cycle control. In a total of 18 genes associated with metabolism, 13 were expressed in blastocysts upon activation and 5 on dormancy [78]. In another investi- gation, D'Souza et al. [79] suggested that genetic instability in the embryos triggers the uptake of energy substrates and ami- no acids to facilitate the DNA repair process. In our study, the amino acid turnover was twice as high in standard cultures than in oviECM cultures, suggesting less stress and better embryo performance on oviECM. Based on the "quiet embryo hypothesis", the oviECM coating conditions appear to support viable early embryos with "quieter" metabolism than embryos cultured under standard conditions [80].

Conclusions

The physical and biochemical environment significantly im- pacts the in vitro growth and development of embryos. Based on this fact, we have implemented a specialized surface for in vitro culture that consists of a decellularized oviductal ECM. We have demonstrated appropriate preservation of the ECM and retention of a specific mixture of biomolecules de- rived from the native microenvironment after biochemical and mechanical treatments. When embryos were cultured on oviECM coating, blastocyst development rates were compa- rable to the current gold standard but with evidence of better metabolic performance, suggesting a quiet metabolism con- sistent with successful embryo development. This could be due to a slow release of specific supportive molecules from the oviECM coating and to the presence of key signalling molecules in it. While more research is needed to assess the impact of this technique on embryos and possible offspring, there is no doubt that tissue engineering has potential within reproductive medicine.

References

1.   Agarwal A, Mulgund A, Hamada A, Chyatte MR. A unique view on male infertility around the globe. Reprod Biol Endocrinol RBE. 2015;13:37. https://doi.org/10.1186/s12958-015-0032-1.
2.   Swain JE, Smith GD. Advances in embryo culture platforms: novel approaches to improve preimplantation embryo development through modifications of the

microenvironment. Hum Reprod Update. 2011;17:541–57. https://doi.org/10.1093/humupd/ dmr006.

3. Carrascosa JP, Horcajadas JA, Moreno-Moya JM. Chapter 15 - The molecular signature of the endometrial receptivity: research and clinical application. In: Horcajadas JA, Gosálvez J, editors. Reproductomics, Academic Press; 2018, p. 279–301. https://doi. org/10.1016/B978-0-12-812571-7.00016-2.

4. Vajta G, Rienzi L, Cobo A, Yovich J. Embryo culture: can we perform better than nature? Reprod BioMed Online. 2010;20: 453–69. https://doi.org/10.1016/j.rbmo.2009.12.018.

5. Mantikou E, Youssef M a. FM, van Wely M, van der Veen F, Al- Inany HG, Repping S, et al. Embryo culture media and IVF/ICSI success rates: a systematic review. Hum Reprod Update 2013;19: 210–220. https://doi.org/10.1093/humupd/dms061.

6. Simopoulou M, Sfakianoudis K, Rapani A, Giannelou P, Anifandis G, Bolaris S, et al. Considerations regarding embryo culture condi- tions: from media to epigenetics. Vivo Athens Greece 2018;32: 451–60. https://doi.org/10.21873/invivo.11261.

7. Young RC, Goloman G. Allo- and xeno-reassembly of human and rat myometrium from cells and scaffolds. Tissue Eng Part A. 2013;19:2112–9. https://doi.org/10.1089/ten.TEA.2012.0549.

8. Santoso EG, Yoshida K, Hirota Y, Aizawa M, Yoshino O, Kishida A, et al. Application of detergents or high hydrostatic pressure as decellularization processes in uterine tissues and their subsequent effects on in vivo uterine regeneration in murine models. PLoS

One. 2014;9:e103201. https://doi.org/10.1371/journal.pone. 0103201.

9. Miyazaki K, Maruyama T. Partial regeneration and reconstruction of the rat uterus through recellularization of a decellularized uterine matrix. Biomaterials. 2014;35:8791–800. https://doi.org/10.1016/j. biomaterials.2014.06.052.

10. Hellström M, Moreno-Moya JM, Bandstein S, Bom E, Akouri RR, Miyazaki K, et al. Bioengineered uterine tissue supports pregnancy in a rat model. Fertil Steril. 2016;106:487–496.e1. https://doi.org/ 10.1016/j.fertnstert.2016.03.048.

11. Raya-Rivera AM, Esquiliano D, Fierro-Pastrana R, López- Bayghen E, Valencia P, Ordorica-Flores R, et al. Tissue- engineered autologous vaginal organs in patients: a pilot cohort study. Lancet Lond Engl. 2014;384:329–36. https://doi.org/10. 1016/S0140-6736(14)60542-0.

12. Greco KV, Jones LG, Obiri-Yeboa I, Ansari T. Creation of an acellular vaginal matrix for potential vaginal augmentation and clo- acal repair. J Pediatr Adolesc Gynecol. 2018;31:473–9. https://doi. org/10.1016/j.jpag.2018.05.003.

13. Liu W-Y, Lin S-G, Zhuo R-Y, Xie Y-Y, Pan W, Lin X-F, et al. Xenogeneic decellularized scaffold: a novel platform for ovary re- generation. Tissue Eng Part C Methods. 2017;23:61–71. https://doi. org/10.1089/ten.tec.2016.0410.

14. Hassanpour A, Talaei-Khozani T, Kargar-Abarghouei E, Razban V, Vojdani Z. Decellularized human ovarian scaffold based on a sodium lauryl ester sulfate (SLES)- treated protocol, as a natural three-dimensional scaffold for construction of bioengineered ova- ries. Stem Cell Res Ther. 2018;9:252. https://doi.org/10.1186/ s13287-018-0971-5.

15. DeQuach JA, Mezzano V, Miglani A, Lange S, Keller GM, Sheikh F, et al. Simple and high yielding method for preparing tissue spe- cific extracellular matrix coatings for cell culture. PLoS One. 2010;5:e13039. https://doi.org/10.1371/journal.pone.0013039.

16. French KM, Boopathy AV, DeQuach JA, Chingozha L, Lu H, Christman KL, et al. A naturally derived cardiac extracellular ma- trix enhances cardiac progenitor cell behavior in vitro. Acta Biomater. 2012;8:4357–64. https://doi.org/10.1016/j.actbio.2012. 07.033.

17. Young DA, Choi YS, Engler AJ, Christman KL. Stimulation of adipogenesis of adult adipose-derived stem cells using substrates that mimic the stiffness of adipose

tissue. Biomaterials. 2013;34: 8581–8. https://doi.org/10.1016/j.biomaterials.2013.07.103.

18.   Zhang X, Dong J. Direct comparison of different coating matrix on the hepatic differentiation from adipose-derived stem cells. Biochem Biophys Res Commun. 2015;456:938–44. https://doi. org/10.1016/j.bbrc.2014.11.004.

19.   Sackett SD, Tremmel DM, Ma F, Feeney AK, Maguire RM, Brown ME, et al. Extracellular matrix scaffold and hydrogel derived from decellularized and delipidized human pancreas. Sci Rep. 2018;8: 10452. https://doi.org/10.1038/s41598-018-28857-1.

20.   Su J, Satchell SC, Shah RN, Wertheim JA. Kidney decellularized extracellular matrix hydrogels: rheological characterization and hu- man glomerular endothelial cell response to encapsulation. J Biomed Mater Res A. 2018;106:2448–62. https://doi.org/10.1002/ jbm.a.36439.

21.   Campo H, García-Domínguez X, López-Martínez S, Faus A, Vicente Antón JS, Marco-Jiménez F, et al. Tissue-specific decellularized endometrial substratum mimicking different physio- logical conditions influences in vitro embryo development in a rabbit model. Acta Biomater. 2019;89:126–38. https://doi.org/10. 1016/j.actbio.2019.03.004.

22.   Catoira MC, Fusaro L, Di Francesco D, Ramella M, Boccafoschi F. Overview of natural hydrogels for regenerative medicine applica- tions. J Mater Sci Mater Med. 2019;30:115. https://doi.org/10. 1007/s10856-019-6318-7.

23.   Crapo PM, Gilbert TW, Badylak SF. An overview of tissue and whole organ decellularization processes. Biomaterials. 2011;32: 3233–43. https://doi.org/10.1016/j.biomaterials.2011.01.057.

24.   Johnson TD, Dequach JA, Gaetani R, Ungerleider J, Elhag D, Nigam V, et al. Human versus porcine tissue sourcing for an inject- able myocardial matrix hydrogel. Biomater Sci. 2014;2014: 60283D–744. https://doi.org/10.1039/C3BM60283D.

25.   Amorim CA. Special issue devoted to a new field of regenerative medicine: reproductive tissue engineering. Ann Biomed Eng. 2017;45:1589–91. https://doi.org/10.1007/s10439-017-1862-0.

26.   Vianello S, Lutolf MP. Understanding the mechanobiology of early mammalian development through bioengineered models. Dev Cell. 2019;48:751–63. https://doi.org/10.1016/j.devcel.2019.02.024.

27.   Fuchs C, Scheinast M, Pasteiner W, Lagger S, Hofner M, Hoellrigl A, et al. Self-organization phenomena in embryonic stem cell- derived embryoid bodies: axis formation and breaking of symmetry during cardiomyogenesis. Cells Tissues Organs. 2012;195:377–91. https://doi.org/10.1159/000328712.

28.   Kolahi KS, Donjacour A, Liu X, Lin W, Simbulan RK, Bloise E, et al. Effect of substrate stiffness on early mouse embryo develop- ment. PLoS One. 2012;7:e41717. https://doi.org/10.1371/journal. pone.0041717.

29.   Morris SA, Grewal S, Barrios F, Patankar SN, Strauss B, Buttery L, et al. Dynamics of anterior-posterior axis formation in the develop- ing mouse embryo. Nat Commun. 2012;3:673. https://doi.org/10. 1038/ncomms1671.

30.   Warmflash A, Sorre B, Etoc F, Siggia ED, Brivanlou AH. A meth- od to recapitulate early embryonic spatial patterning in human em- bryonic stem cells. Nat Methods. 2014;11:847–54. https://doi.org/ 10.1038/nmeth.3016.

31.   Zhao S, Liu Z-X, Gao H, Wu Y, Fang Y, Wu S-S, et al. A three- dimensional culture system using alginate hydrogel prolongs hatched cattle embryo development in vitro. Theriogenology. 2015;84:184–92. https://doi.org/10.1016/j.theriogenology.2015. 03.011.

32.   Yang H, Wu S, Feng R, Huang J, Liu L, Liu F, et al. Vitamin C plus hydrogel facilitates bone marrow stromal cell-mediated endometri- um regeneration in rats. Stem Cell Res Ther. 2017;8:267. https:// doi.org/10.1186/s13287-017-0718-8.

33. Hussey GS, Pineda Molina C, Cramer MC, Tyurina YY, Tyurin VA, Lee YC, et al. Lipidomics and RNA sequencing reveal a novel subpopulation of nanovesicle within extracellular matrix biomate- rials. Sci Adv. 2020;6:eaay4361. https://doi.org/10.1126/sciadv. aay4361.

34. Cramer MC, Badylak SF. Extracellular matrix-based biomaterials and their influence upon cell behavior. Ann Biomed Eng. 2019;48: 2132–53. https://doi.org/10.1007/s10439-019-02408-9.

35. Huleihel L, Hussey GS, Naranjo JD, Zhang L, Dziki JL, Turner NJ, et al. Matrix-bound nanovesicles within ECM bioscaffolds. Sci Adv. 2016;2:e1600502. https://doi.org/10.1126/sciadv.1600502.

36. Gu Z, Guo J, Wang H, Wen Y, Gu Q. Bioengineered microenvi- ronment to culture early embryos. Cell Prolif. 2020;53:e12754. https://doi.org/10.1111/cpr.12754.

37. Ezzati M, Djahanbakhch O, Arian S, Carr BR. Tubal transport of gametes and embryos: a review of physiology and pathophysiolo- gy. J Assist Reprod Genet. 2014;31:1337–47. https://doi.org/10. 1007/s10815-014-0309-x.

38. Fischer B, Chavatte-Palmer P, Viebahn C, Navarrete Santos A, Duranthon V. Rabbit as a reproductive model for human health. Reprod Camb Engl. 2012;144:1–10. https://doi.org/10.1530/REP- 12-0091.

39. Freytes DO, Martin J, Velankar SS, Lee AS, Badylak SF. Preparation and rheological characterization of a gel form of the porcine urinary bladder matrix. Biomaterials. 2008;29:1630–7. https://doi.org/10.1016/j.biomaterials.2007.12.014.

40. Shevchenko A, Jensen ON, Podtelejnikov AV, Sagliocco F, Wilm M, Vorm O, et al. Linking genome and proteome by mass spec- trometry: large-scale identification of yeast proteins from two di- mensional gels. Proc Natl Acad Sci U S A. 1996;93:14440– 5. https://doi.org/10.1073/pnas.93.25.14440.

41. Shilov IV, Seymour SL, Patel AA, Loboda A, Tang WH, Keating SP, et al. The Paragon Algorithm, a next generation search engine that uses sequence temperature values and feature probabilities to identify peptides from tandem mass spectra. Mol Cell Proteomics MCP. 2007;6:1638–55. https://doi.org/10.1074/mcp.T600050- MCP200.

42. Viudes-de-Castro MP, Marco-Jiménez F, Más Pellicer A, García- Domínguez X, Talaván AM, Vicente JS. A single injection of corifollitropin alfa supplemented with human chorionic gonadotro- pin increases follicular recruitment and transferable embryos in the rabbit. Reprod Domest Anim Zuchthyg. 2019;54:696–701. https:// doi.org/10.1111/rda.13411.

43. Diretto G, Rubio-Moraga A, Argandoña J, Castillo P, Gómez- Gómez L, Ahrazem O. Tissue-specific accumulation of sulfur com- pounds and saponins in different parts of garlic cloves from purple and white ecotypes. Mol Basel Switz. 2017;22. https://doi.org/10. 3390/molecules22081359.

44. Cappelli G, Giovannini D, Basso AL, Demurtas OC, Diretto G, Santi C, et al. A Corylus avellana L. extract enhances human mac- rophage bactericidal response against Staphylococcus aureus by increasing the expression of anti-inflammatory and iron metabolism genes. J Funct Foods. 2018;45:499–511. https://doi.org/10.1016/j. jff.2018.04.007.

45. Di Meo F, Aversano R, Diretto G, Demurtas OC, Villano C, Cozzolino S, et al. Anti-cancer activity of grape seed semi-polar extracts in human mesothelioma cell lines. J Funct Foods. 2019;61: 103515. https://doi.org/10.1016/j.jff.2019.103515.

46. Benjamini Y, Hochberg Y. Controlling the false discovery rate: a practical and powerful approach to multiple testing. J R Stat Soc Ser B Methodol. 1995;57:289–300.

47. Naba A, Clauser KR, Ding H, Whittaker CA, Carr SA, Hynes RO. The extracellular matrix: tools and insights for the "omics" era. Matrix Biol. 2016;49:10–24. https://doi.org/10.1016/j.matbio. 2015.06.003.

48. Holm S. A simple sequentially rejective multiple test procedure. Scand J Stat. 1979;6:65–70.

49. Clerc O, Deniaud M, Vallet SD, Naba A, Rivet A, Perez S, et al. MatrixDB: integration of new data with a focus on glycosamino- glycan interactions. Nucleic Acids Res. 2019;47:D376–81. https:// doi.org/10.1093/nar/gky1035.

50. Hynes RO. Extracellular matrix: not just pretty fibrils. Science. 2009;326:1216–9. https://doi.org/10.1126/science.1176009.

51. Kim S-H, Turnbull J, Guimond S. Extracellular matrix and cell signalling: the dynamic cooperation of integrin, proteoglycan and growth factor receptor. J Endocrinol. 2011;209:139–51. https://doi. org/10.1530/JOE-10-0377.

52. Zagris N. Extracellular matrix in development of the early embryo. Micron Oxf Engl 1993 2001;32:427–38. https://doi.org/10.1016/ s0968-4328(00)00011-1.

53. Nelson CM, Bissell MJ. Of extracellular matrix, scaffolds, and sig- naling: tissue architecture regulates development, homeostasis, and cancer. Annu Rev Cell Dev Biol. 2006;22:287–309. https://doi.org/ 10.1146/annurev.cellbio.22.010305.104315.

54. Bonnans C, Chou J, Werb Z. Remodelling the extracellular matrix in development and disease. Nat Rev Mol Cell Biol. 2014;15:786– 801. https://doi.org/10.1038/nrm3904.

55. Leivo I, Vaheri A, Timpl R, Wartiovaara J. Appearance and distri- bution of collagens and laminin in the early mouse embryo. Dev Biol. 1980;76:100–14. https://doi.org/10.1016/0012-1606(80) 90365-6.

56. Poel WE. Preparation of acellular homogenates from muscle sam- ples. Science. 1948;108:390–1. https://doi.org/10.1126/science. 108.2806.390-a.

57. Saldin LT, Cramer MC, Velankar SS, White LJ, Badylak SF. Extracellular matrix hydrogels from decellularized tissues: structure and function. Acta Biomater. 2017;49:1– 15. https://doi.org/10. 1016/j.actbio.2016.11.068.

58. Wu J, Ding Q, Dutta A, Wang Y, Huang Y-H, Weng H, et al. An injectable extracellular matrix derived hydrogel for meniscus repair and regeneration. Acta Biomater. 2015;16:49–59. https://doi.org/ 10.1016/j.actbio.2015.01.027.

59. Paduano F, Marrelli M, White LJ, Shakesheff KM, Tatullo M. Odontogenic differentiation of human dental pulp stem cells on hydrogel scaffolds derived from decellularized bone extracellular matrix and collagen type I. PLoS One. 2016;11:e0148225. https:// doi.org/10.1371/journal.pone.0148225.

60. Keane TJ, Dziki J, Sobieski E, Smoulder A, Castleton A, Turner N, et al. Restoring mucosal barrier function and modifying macro- phage phenotype with an extracellular matrix hydrogel: potential therapy for ulcerative colitis. J Crohns Colitis. 2017;11:360–8. https://doi.org/10.1093/ecco-jcc/jjw149.

61. Wu Y, Wang J, Shi Y, Pu H, Leak RK, Liou AKF, et al. Implantation of brain-derived extracellular matrix enhances neuro- logical recovery after traumatic brain injury. Cell Transplant. 2017;26:1224–34. https://doi.org/10.1177/0963689717714090.

62. Ghuman H, Gerwig M, Nicholls FJ, Liu JR, Donnelly J, Badylak SF, et al. Long-term retention of ECM hydrogel after implantation into a sub-acute stroke cavity reduces lesion volume. Acta Biomater. 2017;63:50–63. https://doi.org/10.1016/j.actbio.2017. 09.011.

63. Badylak SF, Freytes DO, Gilbert TW. Extracellular matrix as a biological scaffold material: structure and function. Acta Biomater. 2009;5:1–13. https://doi.org/10.1016/j.actbio.2008.09. 013.

64. Li S, Winuthayanon W. Oviduct: roles in fertilization and early embryo development. J Endocrinol. 2017;232:R1–26. https://doi. org/10.1530/JOE-16-0302.

65. Campo H, Baptista PM, López-Pérez N, Faus A, Cervelló I, Simón C. De- and recellularization of the pig uterus: a bioengineering pilot study. Biol Reprod. 2017;96:34–45. https://doi.org/10.1095/ biolreprod.116.143396.

66. Jensen CE, Zachariae F. Studies on the mechanism of ovulation: isolation and analysis of acid mucopolysaccharides in bovine fol- licular fluid. Acta Endocrinol. 1958;27:356–68.

67.   Templeton DM. Proteoglycans in cell regulation. Crit Rev Clin Lab Sci. 1992;29:141–84. https://doi.org/10.3109/10408369209114599.

68.   Kano K, Miyano T, Kato S. Effects of glycosaminoglycans on the development of in vitro-matured and -fertilized porcine oocytes to the blastocyst stage in vitro. Biol Reprod. 1998;58:1226–32. https:// doi.org/10.1095/biolreprod58.5.1226.

69.   Jang G, Lee BC, Kang SK, Hwang WS. Effect of glycosaminogly- cans on the preimplantation development of embryos derived from in vitro fertilization and somatic cell nuclear transfer. Reprod Fertil Dev. 2003;15:179–85. https://doi.org/10.1071/rd02054.

70.   Lane M, Maybach JM, Hooper K, Hasler JF, Gardner DK. Cryo- survival and development of bovine blastocysts are enhanced by culture with recombinant albumin and hyaluronan. Mol Reprod Dev. 2003;64:70–8. https://doi.org/10.1002/mrd.10210.

71.   Palasz AT, Rodriguez-Martinez H, Beltran-Breña P, Perez-Garnelo S, Martinez MF, Gutierrez-Adan A, et al. Effects of hyaluronan, BSA, and serum on bovine embryo in vitro development, ultra- structure, and gene expression patterns. Mol Reprod Dev. 2006;73:1503–11. https://doi.org/10.1002/mrd.20516.

72.   Figueiredo F, Jones GM, Thouas GA, Trounson AO. The effect of extracellular matrix molecules on mouse preimplantation embryo development in vitro. Reprod Fertil Dev. 2002;14:443–51. https:// doi.org/10.1071/rd02007.

73.   Adams JC, Watt FM. Regulation of development and differentia- tion by the extracellular matrix. Dev Camb Engl. 1993;117:1183– 98.

74.   Turpeenniemi-Hujanen T, Feinberg RF, Kauppila A, Puistola U. Extracellular matrix interactions in early human embryos: implica- tions for normal implantation events. Fertil Steril. 1995;64:132–8.

75.   Ishihara J, Ishihara A, Fukunaga K, Sasaki K, White MJV, Briquez PS, et al. Laminin heparin-binding peptides bind to several growth factors and enhance diabetic wound healing. Nat Commun. 2018;9: 2163. https://doi.org/10.1038/s41467-018-04525-w.

76.   Uyar A, Seli E. Metabolomic assessment of embryo viability. Semin Reprod Med. 2014;32:141–52. https://doi.org/10.1055/s- 0033-1363556.

77.   Leese HJ, Baumann CG, Brison DR, McEvoy TG, Sturmey RG. Metabolism of the viable mammalian embryo: quietness revisited. Mol Hum Reprod. 2008;14:667–72. https://doi.org/10.1093/ molehr/gan065.

78.   Hamatani T, Daikoku T, Wang H, Matsumoto H, Carter MG, Ko MSH, et al. Global gene expression analysis identifies molecular pathways distinguishing blastocyst dormancy and activation. Proc Natl Acad Sci U S A. 2004;101:10326–31. https://doi.org/10.1073/ pnas.0402597101.

79.   D'Souza F, Pudakalakatti SM, Uppangala S, Honguntikar S, Salian SR, Kalthur G, et al. Unraveling the association between genetic integrity and metabolic activity in pre-implantation stage embryos. Sci Rep. 2016;6. https://doi.org/10.1038/srep37291.

80.   Leese HJ. Quiet please, do not disturb: a hypothesis of embryo metabolism and viability. BioEssays News Rev Mol Cell Dev Biol. 2002;24:845–9. https://doi.org/10.1002/bies.10137.

Fig. 1 Experimental schema. Two types of hydrogels were made (with decellularized tissue and with untreated tissue), and four experimental conditions were analysed at the metabolomic level (CM, CM + OH, CM + E, CM + OH + E). Abbreviations: DAPI, 4′,6-diamidino-2- fenilindol; GAGs, glycosaminoglycans; SEM, scanning electron microscopy; HA, hyaluronic acid; CM, culture medium; OH, oviductal ECM hydrogel; E, embryos
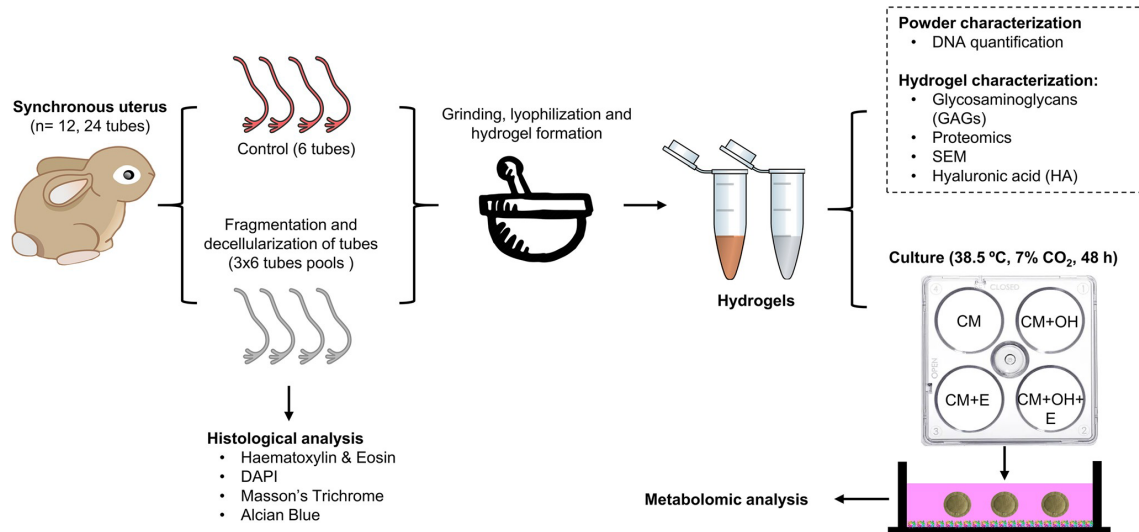
Fig. 2 Assessing rabbit oviduct decellularization and ECM architecture. H&E (a, b) and DAPI (c, d), exhibiting removal of cellular material and complete destruction of nuclei. DNA quantification (i), confirming a 96.75% reduction in double-stranded DNA. Masson's trichrome (e, f) and Alcian blue (g, h) stainings, demonstrating the presence of collagen fibres and partial retention of GAGs after decellularization (data are expressed as the mean ± standard deviation (SD), N = 3 per group; triple asterisks indicate significant differences of $p < 0.001$)
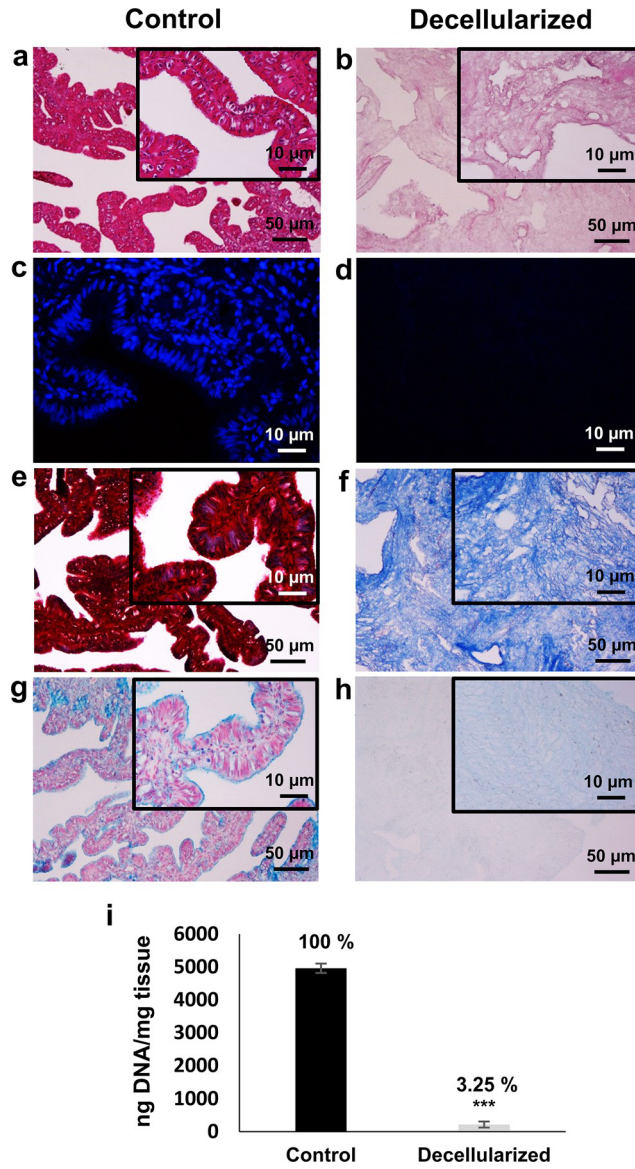
Fig. 3 Ultrastructure and GAG content of hydrogels. SEM images of control (a, c, e and g) and decellularized (b, d, g and h) hydrogels (oviECM), showing both have a very similar complex fibre network. k The average fibre diameters of both hydrogels were similar. oviECM hydrogels had 84.54% less GAGs (i) and 28.68% less HA (j) than control hydrogels (data are expressed as the mean ± standard deviation (SD), N = 3 per group; triple asterisks and single asterisk indicate significant differences of p < 0.001 and p < 0.05, respectively).
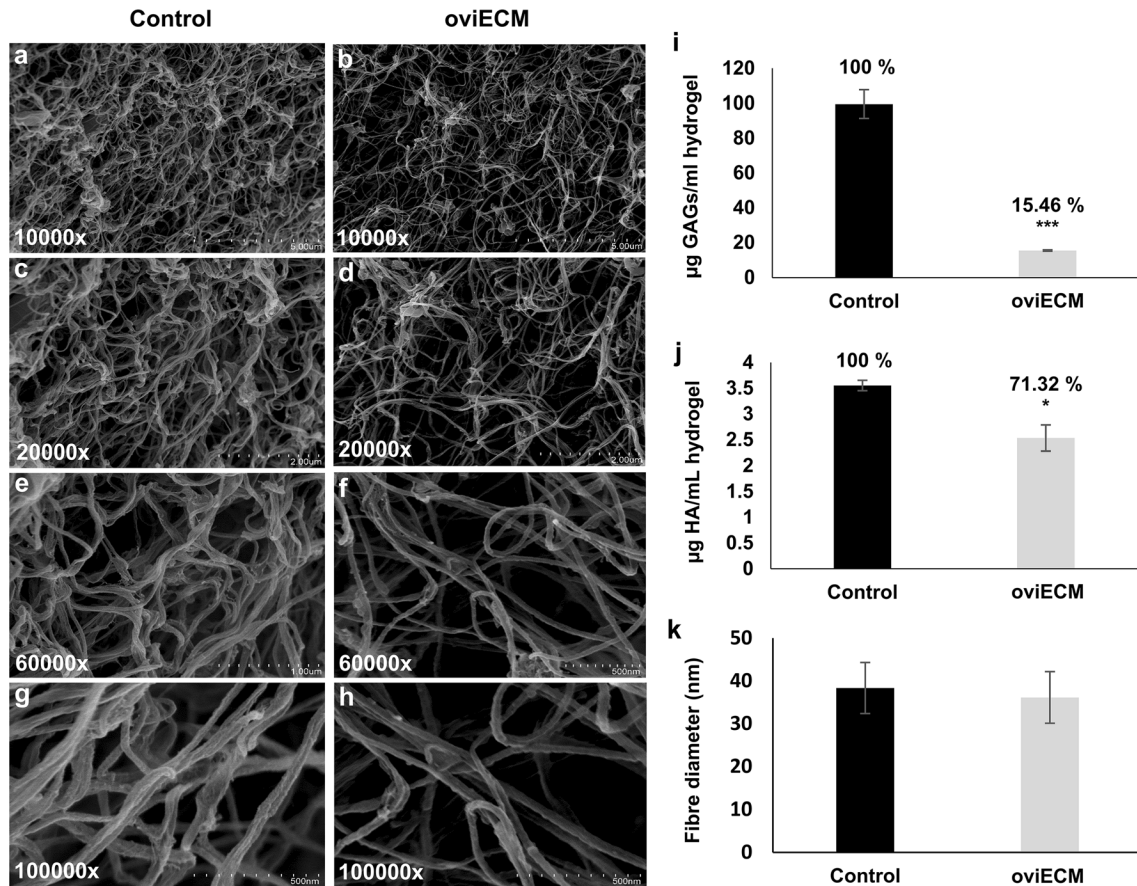
Fig. 4 Proteomic analysis of control and decellularized hydrogels. a SDS-PAGE of the three biological replicates of each hydrogel type. For each sample, 5 gel fragments were processed and analysed separately. b Quantitative heatmap data (native condition = control; decellularized hydrogel = oviECM). c Enrichment analysis of GO terms for proteins with greater abundance in the oviECM hydrogel (blue) or in the control hydrogel (red). N =3 per group
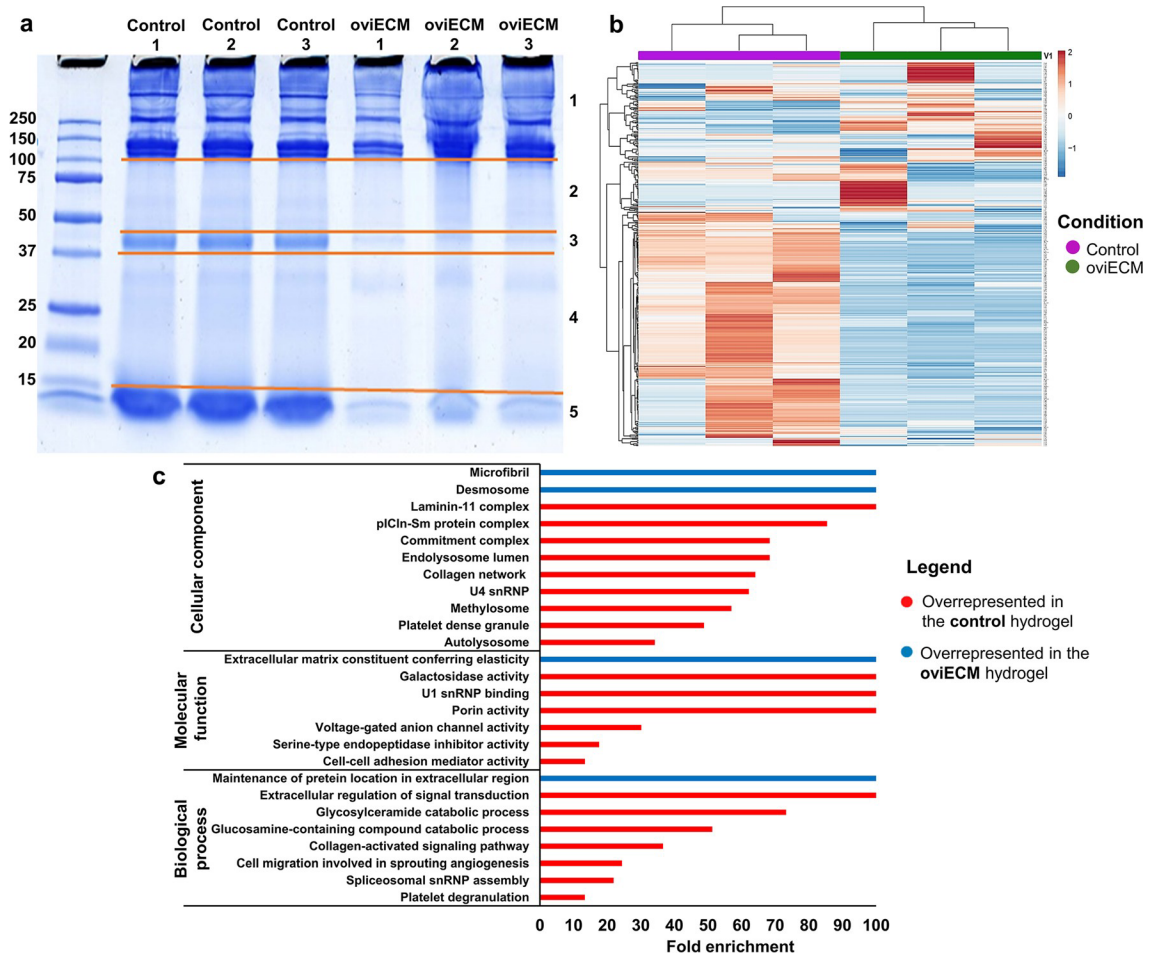
Fig. 5 Matrisomal proteins in control and oviECM hydrogels. a Percentages of proteins within different matrisomal subcategories were calculated by dividing the protein numbers of individual matrisomal subcategories by the total number of extracellular proteins. b Distribution of proteins identified (IDs) in matrisomal classes for oviECM and native hydrogels. Only proteins detected in at least two biological replicates were considered.
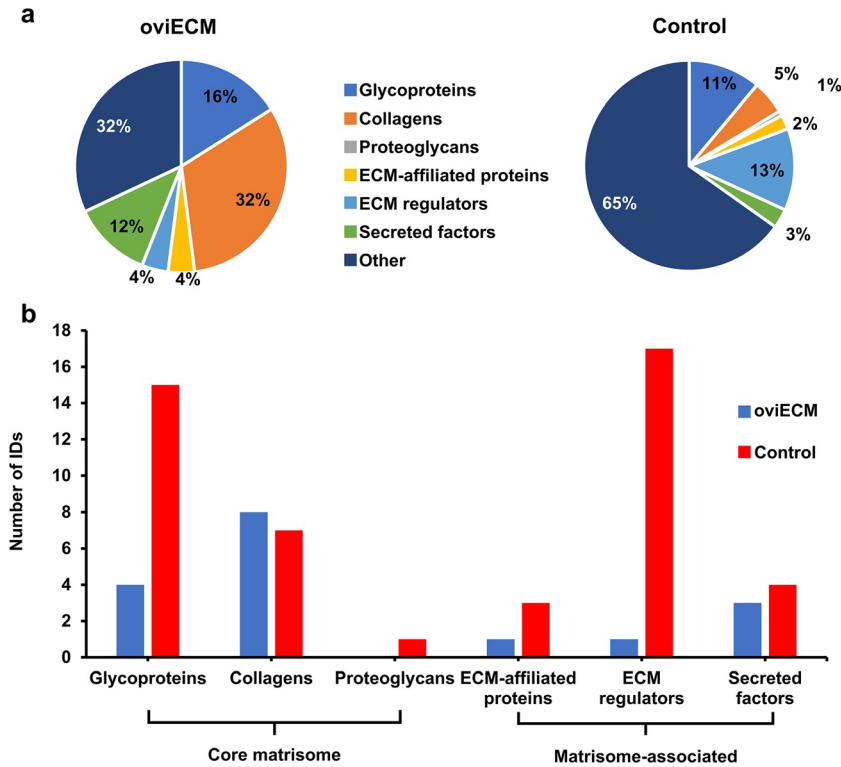
Fig. 6 Untargeted metabolomic analysis of culture media. a Principal component analysis and b heatmaps of 50 untargeted metabolites. c Number of metabolites with significantly different abundances between different conditions (p < 0.05). N =6 per group
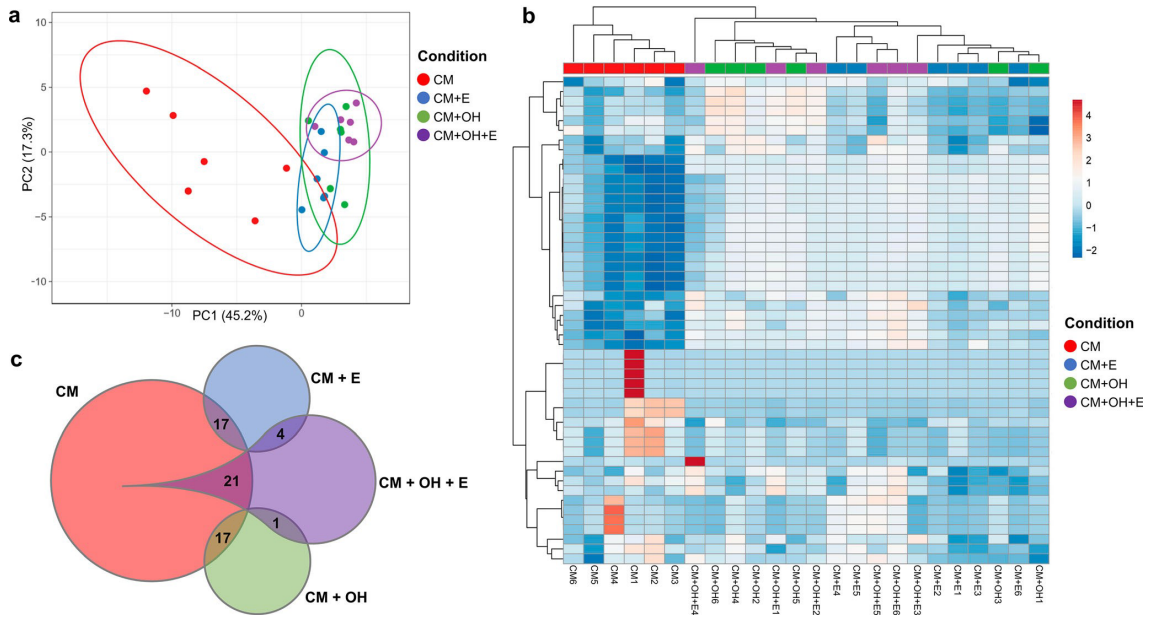
Table 1 Decellularization protocol for fragmented rabbit oviduct

Component	Concentration	Duration
PBS	1×	1 h
SDS	0.1%	22 h
PBS	1×	3 min
Triton X-100	0.5%	2 h
PBS	1×	30 min (×2)
PBS	1×	O/N
DNase I solution	30 µg/ml	4 h
PBS	1×	30 min (×3)

PBS phosphate-buffered saline, *SDS* sodium dodecyl sulphate

Table 2. List of identified matrisomal proteins in control and decellularized (oviECM) hydrogels

Subcategory	Gene name	Protein name	Control	oviECM
Glycoprotein	AGRN	Agrin	x	
Glycoprotein	EFEMP1	EGF-containing fibulin-like extracellular matrix protein 1	x	
Glycoprotein	EMILIN1	Elastin microfibril interfacer 1	x	
Glycoprotein	FBN1	Fibrillin 1	x	x
Glycoprotein	FBN2	Fibrillin 2	x	x
Glycoprotein	FN1	Fibronectin	x	x
Glycoprotein	LAMA2	Laminin subunit alpha 2	x	
Glycoprotein	LAMA5	Laminin subunit alpha 5	x	
Glycoprotein	LAMB1	Laminin subunit beta 1	x	
Glycoprotein	LAMB2	Laminin subunit beta 2	x	
Glycoprotein	LAMC1	Laminin subunit gamma 1	x	x
Glycoprotein	LTBP4	Latent-transforming growth factor beta-binding protein 4	x	
Glycoprotein	SBSPON	Somatomedin B and thrombospondin type 1 domain-containing protein	x	
Glycoprotein	TINAGL1	Tubulointerstitial nephritis antigen-like	x	
Glycoprotein	VWF	von Willebrand factor	x	
Collagen	COL15A1	Collagen alpha-1(XV) chain	x	
Collagen	COL1A1	Collagen alpha-1(I) chain	x	x
Collagen	COL1A2	Collagen alpha-2(I) chain	x	x
Collagen	COL2A1	Collagen alpha-1(II) chain		x
Collagen	COL3A1	Collagen alpha-1(III) chain	x	x
Collagen	COL4A2	Collagen alpha-2(IV) chain	x	x
Collagen	COL4A6	Collagen alpha-6(IV) chain	x	
Collagen	COL5A1	Collagen alpha-2(V) chain		x
Collagen	COL6A2	Collagen alpha-2(VI) chain		x
Collagen	COL6A3	Collagen alpha-3(VI) chain	x	x
Proteoglycan	HSPG2	Basement membrane-specific heparan sulphate proteoglycan core protein	x	
ECM-affiliated	ANXA6	Annexin A6	x	
ECM-affiliated	MUC5AC	Mucin 5AC, oligomeric mucus/gel-forming	x	x
ECM-affiliated	OVGP1	Oviduct-specific glycoprotein	x	
ECM regulator	A2M	Alpha-2-macroglobulin	x	
ECM regulator	CD109	CD109 antigen	x	
ECM regulator	CTSB	Cathepsin B	x	
ECM regulator	CTSC	Dipeptidyl peptidase 1	x	
ECM regulator	CTSZ	Cathepsin Z	x	
ECM regulator	ITIH4	Inter-alpha-trypsin inhibitor heavy chain H4	x	
ECM regulator	ITIH5	Inter-alpha-trypsin inhibitor heavy chain H5	x	
ECM regulator	PLG	Plasminogen	x	
ECM regulator	SERPINA5	Plasma serine protease inhibitor	x	
ECM regulator	SERPINB1	Leukocyte elastase inhibitor	x	
ECM regulator	SERPINB6	Serpin B6	x	
ECM regulator	SERPINB9	Serpin B9	x	
ECM regulator	SERPINC1	Antithrombin III	x	
ECM regulator	SERPINE2	Glia-derived nexin	x	
ECM regulator	SERPINF2	Serpin peptidase inhibitor, clade F, member 2	x	x
ECM regulator	TGM2	Protein-glutamine gamma-glutamyltransferase 2	x	
ECM regulator	TIMP3	Metalloproteinase inhibitor 3	x	
Secreted factor	FLG2	Filaggrin family member 2	x	x
Secreted factor	HRNR	Hornerin	x	x
Secreted factor	MDK	Midkine	x	
Secreted factor	S100A8	S100 calcium-binding protein A8	x	
Secreted factor	S100A9	S100 calcium-binding protein A9		x

Table 3. Changes in the abundance of metabolites in culture media

Metabolic pathway	Metabolite	FC 1	FC 2	FC 3	FC 4
Biosynthesis of amino acids	Asparagine	2.423	1.953	0.093	-0.377
	Arginine	-0.581	-0.586	0.258	0.253
	Aspartate	-1.073	-1.503	0.245	-0.185
	Glutamic acid	-0.514	-0.711	0.204	0.007
	Glycine	-0.283	-1.351	0.747	-0.321
	Histidine	-0.567	-0.506	0.238	0.299
	Isoleucine-leucine	1.037	0.775	0.232	-0.031
	Lysine	-0.568	-0.278	0.350	0.640
	Methionine	-0.384	-0.371	1.388	1.402
	Phenylalanine	2.785	2.715	0.235	0.165
	Tyrosine	2.108	2.062	0.506	0.460
	Tryptophan	0.525	0.757	-0.698	-0.467
	Serine	-0.605	-1.242	0.595	-0.042
	Proline	1.007	0.553	-0.367	-0.821
	Valine	-0.327	0.018	0.144	0.489
Oxidative phosphorylation	Gluconate	1.312	1.324	0.058	0.071
	Glucose	0.815	0.711	0.336	0.231
Glycolisis/Gluconeogenesis	Glucose	0.815	0.711	0.336	0.231
	Glyceraldehyde-3P	-0.652	-1.139	0.659	0.172
	Glycerone-P	-0.793	-0.839	0.342	0.296
	Phosphoenol-pyruvate	-1.053	-0.867	0.193	0.378
Insulin signaling pathway	Glucose	0.815	0.711	0.336	0.231

Numbers in red denote significant differences between the contrasted groups ($p < 0.05$)

FC 1, log-fold change between CM and CM + E groups; *FC 2*, log-fold change between CM and CM + OH groups; *FC 3*, log-fold change between CM + OH and CM + OH + E groups; *FC 4*, log-fold change between CM + E and CM + OH + E groups